Stochastic Approach to Estimating Stresses of Polymer Films from the Surface Microprofile

A.M. Pashayev, A.Kh. Janahmadov
National Aviation Academy of Azerbaijan (Mardakan ave, 30, Baku, AZ1045, Azerbaijan)

For correspondence:
Janahmadov Ahad / e-mail: dzhanakhmedov@yahoo.com

Abstract

The existing methods for determining the internal (residual, shrinkage) stresses arising from the curing of thin films of paint and varnish coatings (PVC), based on the cantilever bending of the substrate and the difference in the thicknesses of the wet and dry coatings, are analyzed. The dependence of their accuracy on the film / substrate thickness ratio and the uniformity of the applied film is noted. The application of atomic force microscopy methods based on measuring the geometry of the regular microrelief (RMR) of the film surface, which serves as a characteristic manifestation of its shrinkage deformations, is considered. It is noted that when applying the Euler problem on the stability of a compressed rod, the method demonstrates the calculated stress values unattainable for most polymers. The calculation of internal stresses and strains was carried out on the basis of a stochastic approach, taking into account the "checkerboard" distribution of deformation defects on the outer surface of the film. On the example of RMR film of polyester urethane varnish, the level of internal stresses was assessed using the proposed and existing methods. The values of internal stresses obtained by the three methods relatively coincide with each other, the difference between them does not exceed ~20%.

Keywords: paint and varnish coating (PVC), substrate, regular microrelief (RMR), shrinkage, shrinkage stresses, internal stresses, curing, polyester urethane varnish, thin film.

DOI: 10.52171/2076-0515_2021_13_02_7_26

For citation:
Pashayev A.M., Janahmadov A.Kh.
[Stochastic Approach to Estimating Stresses of Polymer Films from the Surface Microprofile]
Herald of the Azerbaijan Engineering Academy, 2021, vol. 13, № 2. Pp. 7 –26 (in English).

Polimer plyonkaların səthin mikroprofili üzrə gərginliyinin qiymətləndirilməsinə stoxastik yanaşma

A.M. Paşayev, Ə.X. Canəhmədov
Azərbaycan Milli Aviasiya Akademiyası (Mərdəkan pr. 30, Bakı, AZ1045, Azərbaycan)

Yazışma üçün:
Canəhmədov Əhəd / e-mail: dzhanakhmedov@yahoo.com

Annotasiya

Lak-boya örtüklərinin (LBÖ) nazik plyonkalarının sərtləşməsi zamanı yaranan, müvafiq olaraq, alt qatın konsol əyilməsinə, həmçinin yaş və quru səthlərin qalınlıqlarının fərqinə əsaslanan daxili (qalıq, büzülmə) gərginliyin təyin olunmasının mövcud üsulları təhlil olunub. Onların dəqiqliyinin plyonkanın/alt qatın qalınlığı nisbətindən və plyonkanın bərabərliyindən asılılığı qeyd olunub. Plyonkanın səthinin büzülmə deformasiyalarının xarakterik təzahürü kimi xidmət edən müntəzəm mikrorelyefinin (MMR) həndəsi parametrlərinin ölçülməsinə əsaslanan atom-qüvvə mikroskopu metodu ilə tətbiqinə baxılıb. Qeyd olunub ki, sıxılmış çubuğun dayanıqlığı haqda Eyler məsələsinin tətbiqi zamanı bu metod əksər polimerlər üçün əlçatmaz hesab olunan gərginliyin hesablanmış qiymətini nümayiş etdirir. Daxili gərginliyin və deformasiyanın hesablanması plyonkanın xarici səthində deformasiya nöqsanlarının "şahmat" paylanmasını nəzərə alaraq, stoxastik yanaşma əsasında aparılıb. Poliefiruretan boyanın MMR plyonkalar nümunəsində təklif olunan və mövcud metodlardan istifadə edilərək daxili gərginlik səviyyəsinin qiymətləndirilməsi aparılıb. Hər üç metodla alınan daxili gərginlik kəmiyyətlərinin qiymətləri, bir-biri ilə nisbətən uyğun gəlir, onlar arasındakı fərq ~20% həddindədir.

Açar sözlər: lak-boya örtüyü, alt qat, müntəzəm mikrorelyef, büzülmə, büzücü gərginlik, daxili gərginlik, sərtləşmə, poliefiruretan boya, nazik plyonka.

DOI: 10.52171/2076-0515_2021_13_02_7_26

УДК: 539.219.2

Стохастический подход к оценке напряжений полимерных плёнок по микропрофилю поверхности

А.М. Пашаев, А.Х. Джанахмедов
Национальная авиационная академия Азербайджана (Мардакянский просп., 30, Баку, AZ1045, Азербайджан)

Для переписки:
Джанахмедов Ахад / e-mail: dzhanakhmedov@yahoo.com

Аннотация

Проанализированы существующие методы определения внутренних (остаточных, усадочных) напряжений, возникающих при отверждении тонких плёнок лакокрасочных покрытий (ЛКП), основанные на консольном изгибе подложки и разности толщин мокрого и сухого покрытия, соответственно. Отмечена зависимость их точности от соотношения толщин плёнка/подложка и однородности нанесённой плёнки. Рассмотрено применение методов атомно-силовой микроскопии, основанных на измерении геометрии регулярного микрорельефа (РМР) поверхности плёнки, служащего в качестве характерного проявления её усадочных деформаций. Отмечено, что при применении задачи Эйлера об устойчивости сжатого стержня метод демонстрирует недостижимые для большинства полимеров расчётные значения напряжения. Расчет внутренних напряжений и деформаций проведен на основе стохастического подхода с учетом «шахматного» распределения деформационных дефектов на наружной поверхности пленки. На примере РМР плёнки полиэфируретанового лака проведена оценка уровня внутренних напряжений с использованием предлагаемой и существующих методик. Значения величин внутренних напряжений, полученные по трём методам, относительно совпадают друг с другом, разница между ними не превышает ~20%.

Ключевые слова: лакокрасочное покрытие, подложка, регулярный микрорельеф, усадка, усадочные напряжения, внутренние напряжения, отверждение, полиэфируретановый лак, тонкая плёнка.

Introduction

Protective paint and varnish coatings (PVC) of external surfaces of aircraft (AC) in the process of application and operation undergo a significant mechanical impact, weakening the strength of the film and can lead to a violation of its continuity.

During hardening of PVC, the paintwork goes through the shrinkage (contraction) as a result of the evaporation of volatile components, polymerization, gelation, temperature drops and other processes. The adhesion contact and microroughness of the relief of a rigid substrate do not allow the polymer film to freely shrink ("shrink"), as a result of which it shrinks in thickness and internal tensile stresses arise in it [1].

All this creates a number of problems associated with ensuring the strength and durability of protective coatings. Numerous publications of domestic and foreign authors are devoted to the study of the processes developing in the "substrate - coating" system ("flexible base - thin film", etc.), among which the works of *V.Ye. Panin* [2], and *J.Hutchinson* [3] et al.

The internal (synonyms - residual, shrinkage) stresses sharply weaken the cohesive and adhesive strength of the newly formed film, thereby accelerating the destructive physicochemical processes that cause its premature destruction during operation [4, 5, 6, 7].

Since the internal stresses largely determine the final morphology and properties of the coating and do not depend on the nature of the substrates [8], the assessment of their level is of theoretical and practical interest.

A number of methods for determining shrinkage stresses in thin-film structures on rigid substrates are currently known. One of the first was the proposed method developed independently by *A.T. Sanzharovsky* and *E. Korkoran* and based on the calculation of stresses in the coating by the magnitude of deformations (deflection) of the substrate (cantilever bending tape) [9, 10, 11].

As a result, these works formed the basis of GOST 13036-67 (currently not valid according to IUS 7-77) [12] and its current American analogue ASTM D6991-05 [13].

Purpose of work is to develop and test a method for determining the level of shrinkage stresses in curried PVC based on the characteristics of its microrelief and its comparison with the values obtained using existing techniques. A preliminary analysis of linear disturbances is carried out, which determines the kinetics and energetics of the corrugation process, as well as the amplitude and wavelength of steady-state oscillations.

Due to the uncontrollability of external conditions affecting the properties of the sample, a stochastic approach was used to calculate the internal stresses and strains, taking into account the features of the film – substrate interface.

Problem Statement

In this regard, the authors analyzed the kinetics and energetics of growth of film disturbances as a result of the effect of loading the substrate on the deformation of the film prior to its solidification through the interface through a viscoelastic layer lying directly under the film. As a result, by measuring the geometry of the RMR, the critical values of the parameters of the film vibrations are estimated, at which the vibrations acquire stability with the corresponding steady-state values of the amplitude and wavelength [14].

The cured thin polymer film is taken to be the surface layer of the bulk of the substrate material with a surface layer / substrate interface thickness equal to the film thickness. The loaded solid body of the substrate induces a "checkerboard" distribution of stresses and strains through the film / substrate interface, carrying deformation defects to the film surface. To calculate normal and tangential stresses, a stochastic approach was used, taking into account the conditions for the formation of nonlinear waves of localized plastic flow of the parameters of the elements of the system under consideration at the meso and microscale levels.

Materials and existing methods for calculating internal stresses

A two-component polyether urethane (PEU) varnish ($E = 30\ MPa$, $\mu = 0.35$ [15]) was chosen as the PVC under study. The varnish components (polyester and hardener) were mixed before application and applied to a substrate (plate $102 \times 12 \times 0.254mm$ made of 08X18H10T steel, $E = 1.96 \times 10^5 MPa$, $\mu = 0.29$ [16]) according to the manufacturer's instructions.

The thickness of the film before and after curing was measured in accordance with [17, 18, 19], respectively. Based on the data obtained by methods [12] and [13], using formulas (1) and (2), the internal stresses in the PVC were calculated.

To determine the internal stresses by the proposed method, the RMR of the surface of the hardened film was investigated on an AFM SOLVER NEXT (NT-MDT, Russia). The measurement was carried out by line-by-line scanning of a surface area 50 × 50 μm in size, as a result, two- and three-dimensional topographic images are formed, a profilogram is automatically calculated. As a sample, a fragment of $5 \times 5 \times 0.254mm$ in size was used, cut from the above steel plate after conducting research according to the methods [12, 13].

The essence of the technique lies in the fact that the coating is applied to one surface of a flat sample (tape), which is cantilever clamped in a rigid fixation. During the drying process, internal stresses arise in the coating, as a result of which the free end of the cantilever deviates from its original position by an amount d (deflection).

The calculation of internal stresses is usually carried out according to the following formula:

$$\sigma = \frac{dE_S t^3}{3L^2 c(t+c)(1-\mu_S)} + \frac{dE_C(t+c)}{L^2(1-\mu_C)} \qquad (1)$$

where d – the deflection (deflection) of the free end of the console; E_s – Young's modulus of the steel substrate; μs is the Poisson's ratio of the steel substrate; L – the length of the console; t is the thickness of the console; c – a coating thickness; E_c – Young's modulus of the hardened coating; μ_c – Poisson's ratio of the coating material.

As follows from formula (1), in order to calculate internal stresses, the cantilever method requires knowledge of eight Parameters of the film and substrate (cantilever deflection, geometric dimensions of the substrate, mehanical characteristics).

The cantilever method is applicable for films with a thickness of $25\ldots380\mu m$. The accuracy of the method is highly dependent on the film / substrate ratio and the uniformity of the applied film. Some difficulty of such measurements lies in the fact that, in addition to the shrinkage of the paintwork, the deflection of the tape-console is affected by such a difficult factor as the weight of the coating itself, which gradually decreases as it dries.

Compared with this method, a more simplified formula was proposed in [14] to determine internal stresses in coatings:

$$\sigma = \frac{E(h_0 - h_1)}{h_0} \quad (2)$$

where h_0 – the initial "wet" film thickness; h_1 – a film thickness after curing; E – Young's modulus of the hardened coating.

The thickness of the cured film h_1 is determined according to the standards [17] by microscopic examination of the cross section. Accurate measurement of the initial ("wet") h_0 thickness of a thin layer of paint and varnish material (PVM)[1] presents some difficulty. The existing methods for determining the thickness of "wet" polymer films [18, 19] prescribe direct measurements using a probe instrument in the form of a toothed plate – Rossman's "comb". The protrusions (teeth) of the "comb" are immersed in the layer of the liquid film until they touch the substrate. The height of the wetted edge of the teeth is considered equal to the thickness of the coating. However, already in the description of these methods, it is noted that they are approximate, and on substrates with an uneven or textured surface, they may give erroneous readings.

In accordance with [20], for the paintwork of external surfaces, the R_z value (the sum of the average absolute values of the heights of the five largest profile protrusions and the depths of the five largest profile valleys) with a base length of $2.5mm$ should be less than $0.001mm$ ($1\mu m$), i.e., the surface should have meso- and micro-scale irregularities.

According to the operational requirements [21, 22], the thickness of the cured paintwork must be at least 20% higher than the maximum height of the microroughness of the substrate. If this requirement is met, the film under conditions of adhesive contact is no longer an equidistant surface copy of the smoothed microgeometry of the substrate but has its own regular microrelief (RMR) [23, 24, 25], formed under the action of deformation processes.

Currently, SIEBIMM-methods[2] for studying the mechanical properties of films have become widespread, involving the measurement of the geometric characteristics of their surface using atomic force microscopy (AFM). The appearance of RMR of thin films is considered by some authors on the basis of the Euler problem on the stability of a compressed rod: under a critical load, the film surface bends in the form of sinusoids with a period λ and an amplitude A [26, 27, 28, 29, 30, 31, 32].

In the same works, it is noted that the wavelength of the folds does not depend on the magnitude of stresses, is determined by the characteristics of the film and substrate and is a constant value for a particular pair of materials "film – substrate". In this case, the amplitude of the folds A does not depend on the elastic properties of the film and substrate but increases with increasing compressive stresses [33].

For films adhering to the substrate, wrinkling can occur only when the critical compressive stress σ_w is exceeded:

$$\sigma_w = \frac{E_f'}{4}\left(\frac{3E_s'}{E_f'}\right)^{\frac{2}{3}} \quad (3)$$

where $E_f' = {E_f}/{1-\mu_f^2}$ and $E_s' = {E_s}/{1-\mu_s^2}$

[1] The difference between paints and varnishes materials (PVM) and paints and varnishes coatings (PVC) is to some extent conditional and suggests that the former determine the physicochemical properties, the latter – the geometric size and mechanical properties of the layer.

[2] SIEBIMM – strain-induced elastic buckling instability for mechanical measurements

are the moduli of longitudinal elasticity, E_f, μ_f, E_s, μ_s are Young's moduli and Poisson's ratios of the film and substrate, respectively.

When the compressive stress σ exceeds σ_w, the film spontaneously bends, forming a periodic distribution of folds on the surface.

However, this explanation of relief formation presupposes loading by external horizontal loads, which cause the loss of stability of the already hardened film. But since the modulus of longitudinal elasticity of even hardened paintwork materials PVM (E_f') is approximately three orders of magnitude lower than that of a metal substrate (E_s'), the stresses σ_w calculated by formula (3) will have values unattainable for most polymers, several times exceeding their ultimate strength. In this regard, this model of relief formation is inapplicable for paintwork PVC.

Apparently, from the moment the paintwork material is applied to the substrate, due to the viscoelastic transition from the liquid state to the solid state, the density of the upper layer increases, and an elastic surface film gradually forms, which impedes the further exit of the vapor-gas mixture from the underlying layer of paintwork materials PVM. Based on this, the paintwork PVC at the initial stage of curing can be represented as a two-layer system consisting of a thin elastic surface layer and an underlying deep viscoelastic layer [34, 35].

Probably, evaporating steam-gas flows, locally uplifting the elastic film during mass transfer, create internal stresses in it, forming a characteristic folded surface with a "checkerboard" effect of regular alternation of convex and concave zones [28]. The meso-substructure of the extruded material appears on the surface. According to the classification of scale levels, adopted in the works of V.E. Panin's school [2], the mesoscopic scale level is subdivided into mesoscale-1 $(0.1 - 10\mu m)$ and mesoscale-2 $(10 - 500\mu m)$ [29].

Proposed approach to solving the problem

We consider the deformation of the cured top layer of the paint and varnish coating on the uncured bottom layer as a coherent deformation of an elastic film on a viscoelastic underlayer. As is known [36, 37], in this case, the parameters of folds are largely determined by the kinetics of their formation and growth. The mechanism of the wrinkling process formed by the layer underlying the film is usually interpreted as a stress-induced instability, similar to the buckling of an elastic bar under compression. If this layer has elasticity, then there is a critical compressive stress, above which the film begins to corrugate with the corresponding wavelength obtained by minimizing the total elastic energy of the film and substrate [38, 39, 40]. Under typical compressive stress, corrugations are formed only when the substrate is significantly softer than the film. If the substrate is elastic, then the corrugation becomes a kinetic process [40, 41, 42]. Since the viscous substrate does not have a reserve of elastic energy, the upper surface of the compressed covering film is always energetically unstable. The viscous flow on the substrate regulates the kinetics of corrugation growth by choosing the most growing wavelength. More generally, when the substrate is viscoelastic (for example, crosslinked polymers), both energy and kinetics play an important role. The spectrum of formed corrugated patterns experimentally observed in metal - polymer bilayers [43] demonstrates the features of the kinetic process. Analysis of linear perturbations shows that the viscoelastic property of the substrate has a significant contribution to the stability and kinetics of the corrugation process [37].

Let us consider the process of modeling the evolution of corrugation in a thin elastic - viscoelastic bilayer described in [36] in the limiting case of analysis of linear perturbations. The generated model is based on the application of the nonlinear theory of Karman plates [44] to the elastic layer and the approximation of the viscoelastic layer using a thin layer. Although the model is applicable to 2D corrugation, the focus will be on one-dimensional corrugation under in-plane stress.

Consider an elastic film of thickness h_f resting on a viscoelastic layer of thickness H, which, in turn, lies on a rigid substrate in Fig. 1 [36].

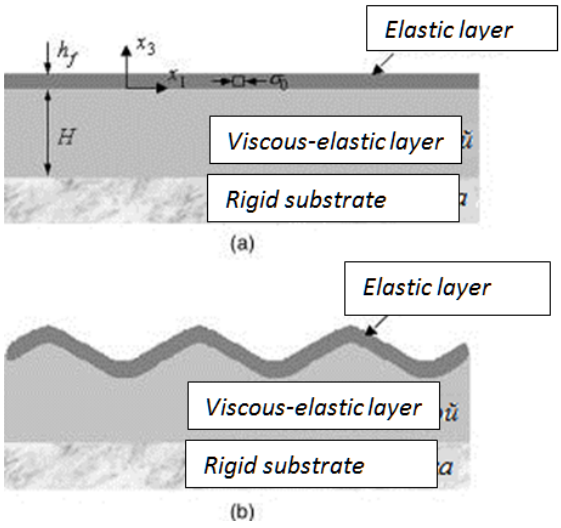

Figure 1 – The schematic of an elastic-viscous bilayer on a rigid substrate: (a) standard state and (b) wrinkling state

In the initial state (Fig.1a), both layers have a flat shape, and the elastic layer is subjected to biaxial residual stress, and there are no traces on the bilayer surface. In the wrinkling state (Fig.1b), both in-plane displacements and out-of-plane displacements occur in the elastic layer caused by the residual stress σ_0 ($\sigma_0 < 0$), while the viscoelastic layer is simultaneously deformed. In Fig.1(a) $x_1 - x_2$ denotes a plane in a rectangular Cartesian coordinate system that serves as an interface between two layers in a bilayer.

Linear analysis of disturbances

The elastic film model will be formulated on the basis of Karman's nonlinear theory of bending of elastic plates [44]. Elastic deformations of the film are characterized by bulging (lateral deflection) w and displacement u_α along the plane ($\alpha = 1.2$).

Suppose the viscoelastic layer experiences slight deflection from the horizontal position

$$w(x,t) = A(t)coskx \tag{4}$$

with amplitude $A(t)$ and length $L = 2\pi/k$ (k – a wave number). In the analysis of linear perturbations, the evolution of displacements in the plane is not associated with swelling (lateral deflection).

It is assumed that the layer on which the film directly rests is isotropic and linearly viscoelastic. According to the theory of viscoelasticity [45], the stress-strain relation is written in the integral form.

$$\sigma_{\alpha\beta}(t) = 2\int_{-\infty}^{t}\mu(t-\tau)\frac{\partial\varepsilon_{\alpha\beta}(\tau)}{\partial\tau}d\tau + \\ +\delta_{\alpha\beta}\int_{-\infty}^{t}\lambda(t-\tau)\frac{\partial\varepsilon_{\gamma\gamma}(\tau)}{\partial\tau}d\tau \tag{5}$$

where $\mu(t)$ and $\lambda(t)$ – the viscoelastic relaxation modules $\delta_{\alpha\beta}$ – the Kronecker symbol. The $\alpha\beta\gamma$ indices take values 1 and 2; repetition of the index in (5) means the summation over 1 and 2. Under the assumption that there is no external force, neglecting the inertia of quasi-static deformation, the equilibrium condition can be written in the form [37]:

$$\frac{\partial\sigma_{\alpha\beta}}{\partial x_\beta} = 0. \tag{6}$$

For small deformations, the strain - displacement relation takes the form:

$$\varepsilon_{\alpha\beta} = \frac{1}{2}\left(\frac{\partial u_\alpha}{\partial x_\beta} + \frac{\partial u_\beta}{\partial x_\alpha}\right). \quad (7)$$

The viscoelastic layer is not loaded at the initial moment of time $(t = 0)$ and undergoes normal and shear displacements on its upper surface at $t > 0$:

$$\sigma_{33} = S_3(x_1, x_2, t)\ and\ \sigma_{3,\alpha} +$$
$$= S_\alpha(x_1, x_2, t) \quad at\ \ x_3 = 0. \quad (8)$$

There are no displacements on the bottom surface of this layer:

$$u_\alpha = u_3 = 0 \quad at\ \ x_3 = -H. \quad (9)$$

In the general case, the surface of the viscoelastic layer undergoes both in-plane and out-of-plane displacements, which are interconnected with each other and only in two special cases they may not have a connection. In the first case, when the viscoelastic layer has a very large thickness ($kH \to \infty$) and is incompressible ($\nu = 0.5$). This case is considered in detail in [37]. In the second case, when this layer is very thin ($kH \to 0$); it is this case that is most typical for paints and varnishes (PVC) and will be described in detail below.

For the relaxation modulus $\mu(t)$, the Kelvin model of linear viscoelasticity will be used, which is a mechanical analogue of a device consisting of a spring and a parallel acting shock absorber

$$\mu(t) = \mu_\infty + \eta \cdot \delta(t), \quad (10)$$

where μ_∞ – the stiffness of the spring, representing the elastic shear modulus with the rubberized limit position; η – viscosity.

The interface between elastic and viscoelastic layers is maintained at each deformation. Consequently, the displacements and their traces remain continuous at the interface that connects the equations of equilibrium of the elastic layer with the time-dependent responses of the viscoelastic layer, which leads to the equations:

$$\frac{\partial w}{\partial t} = \frac{1-2\nu}{2(1-\nu)} \cdot \frac{H}{\eta}\left(-D_f \frac{\partial^4 w}{\partial x_\alpha \partial x_\alpha \partial x_\beta \partial x_\beta} + \right. \quad (11)$$
$$\left. + N_{\alpha\beta}\frac{\partial^2 w}{\partial x_\alpha \partial x_\beta} + \frac{\partial N_{\alpha\beta}}{\partial x_\beta} \cdot \frac{\partial w}{\partial x_\alpha}\right) - \frac{\mu_\infty}{\eta} w$$

$$\frac{\partial u_\alpha}{\partial t} = \frac{H}{\eta} \cdot \frac{\partial N_{\alpha\beta}}{\partial x_\beta} - \frac{\mu_\infty}{\eta} u_\alpha, \quad (12)$$

Where

$$D_f = \frac{E_f \cdot h^3}{12\left(1-\nu_f^2\right)},\ \ N_{\alpha\beta} = \sigma_0 h_f \delta_{\alpha\beta} +$$
$$+ \frac{E_f h_f}{1-\nu_f^2}\left[\left(1-\nu_f\right)\varepsilon_{\alpha\beta} + \nu_f \varepsilon_{\gamma\gamma}\delta_{\alpha\beta}\right] \quad (13)$$

Equations (11) and (12) are interrelated nonlinear evolution equations that can be solved numerically by simulating three-dimensional deformations of an elastic - viscoelastic bilayer and the evolution of the resulting two-dimensional corrugated patterns. For simplicity, we will analyze in detail only the deformations from in-plane compression (tension) and one-dimensional corrugations. Equations (11) – (12) in this case take the form:

$$\frac{\partial w}{\partial t} = \frac{1-2\nu}{2(1-\nu)} \cdot \frac{H}{\eta}\left(-D_f \frac{\partial^4 w}{\partial x^4} + \right. \quad (14)$$
$$\left. + N\frac{\partial^2 w}{\partial x^2} + \frac{\partial N}{\partial x} \cdot \frac{\partial w}{\partial x}\right) - \frac{\mu_\infty}{\eta} w,$$

$$\frac{\partial u}{\partial t} = \frac{H}{\eta} \cdot \frac{\partial N}{\partial x} - \frac{\mu_\infty}{\eta} u, \quad (15)$$

where

$$N = \sigma_0 h_f + \frac{E_f h_f}{1-\nu_f^2}\left[\frac{\partial u}{\partial x} + \frac{1}{2}\left(\frac{\partial w}{\partial x}\right)^2\right] \quad (16)$$

Substituting (4) into (14) and leaving only the leading terms containing the small parameter $A(t)$, we obtain the equation:

$$\frac{dA}{dt} = \frac{\alpha E_f - \mu_\infty}{\eta} A(t), \quad (17)$$

Where

$$\alpha = \frac{(1-2\nu)k^2 H h_f}{24(1-\nu)(1-\nu_f^2)} \left[-k^2 h_f^2 - \frac{12(1-\nu_f^2)\sigma_0}{E_f}\right] \quad (18)$$

The solution to equation (17) is represented in the form

$$A(t) = A_0 exp\left(s \cdot \frac{t}{\tau}\right), \quad (19)$$

where A_0 is the initial amplitude of the disturbance; $\tau = \eta/E_f$ is the characteristic time scale and $s = \alpha - \mu_\infty/E_f$ is the dimensionless growth order of the disturbance. The stability of the bilayer depends on the sign of the parameter s. If $s < 0$ for all wave numbers k, then the bilayer is stable and remains flat. Otherwise, when $s > 0$ for any admissible wavenumbers, the bilayer is unstable and the disturbances grow, forming corrugations. In this case, the amplitude grows exponentially with time in the initial stage. As shown in [37], the initial stage of growth can be non-exponential if the viscoelastic layer has a finite elastic modulus in the glassy state (elastic limit as $t \to 0$).

The growth order of s depends on the disturbance wavelength ($L = 2\pi/k$) for various ratios μ_∞/E_f. In the limiting case, when $\mu_\infty = 0$, we have $s = \alpha$ and $s > 0$ (taking into account $\sigma_0 < 0$) throughout the entire length of the disturbance waves. Therefore, for $s > 0$, the bilayer will be unstable. The critical value of the wavelength corresponding $to\ s \to +0$ is

$$L_c = \pi h_f \sqrt{-\frac{E_f}{3(1-\nu_f^2)\sigma_0}}, \quad (20)$$

which coincides with the critical length of the Euler bend. The growth order is positive for $L > L_c$ and has a peak at the wavelength

$$L_m = \pi h_f \sqrt{-\frac{2E_f}{3(1-\nu_f^2)\sigma_0}}. \quad (21)$$

As the ratio μ_∞/E_f increases, the value of s decreases without changing the shape of the dependence on the normal wavelength L/h_f. As a result, we obtain the second critical value of the wavelength determined by formula (21). The growth order of s remains positive when L changes in the interval between these two critical values. On the other hand, the fastest growth of the wavelength does not change, but the corresponding order of growth of s drops to zero when the value of L approaches the boundaries of this interval from the inside at the critical value of the ratio μ_∞/E_f corresponding to the equality $s = +0$:

$$\left(\frac{\mu_\infty}{E_f}\right)_c = \frac{3(1-\nu_f^2)(1-2\nu)}{2(1-\nu)} \frac{H}{h_f} \left(\frac{\sigma_0}{E_f}\right)^2, \quad (22)$$

whence we find the critical value σ_0^c of the compressive stress, below which the bilayer becomes stable:

$$\sigma_0^c = E_f \left(\alpha \frac{h_f}{H} \frac{2(1-\nu)}{3(1-\nu_f^2)(1-2\nu)}\right)^{1/2} \quad (23)$$

The bilayer becomes stable when μ_∞/E_f is greater than the critical value (22). According to the criticality condition (22), the stability of an elastic – viscoelastic bilayer depends on the elasticity modulus (i.e., on the extended limit of the relaxation modulus μ_∞)

of the viscoelastic layer but does not depend on the initial modulus (i.e., on the glassy state). In other words, despite the initial high viscosity or even stiffness of the viscoelastic layer, the bilayer "foresees" the subsequent softening of the layer and becomes spontaneously unstable. The time scale of the corrugation growth is proportional to the viscosity, and the order of growth increases with decreasing elasticity modulus. The wavelength of the fastest growing mode, however, does not depend on the viscoelastic layer, as follows from (21). As shown in [37], the wavelength of the rapidly growing growth is weakly dependent on the thickness ratio H/h_f and Poisson's ratio. The approximation using a thin layer leads to good accuracy in determining the wavelength but underestimates the order of growth of the fast-growing mode when the thickness ratio H/h_f is greater than 2.

Setting $\partial/\partial t = 0$ in equations (14) and (15), we obtain two coupled nonlinear ordinary differential equations, each of which can be solved in the case of an equilibrium state. First of all, we note that the equilibrium amplitude of a sinusoidal corrugation with a wave number k is given by the expression

$$A_{eq} = \frac{2\sqrt{1-\nu_f^2}}{k}\left[-\frac{\sigma_0}{E_f} - \frac{(kh_f)^2}{12(1-\nu_f^2)} - \right.$$
$$\left. - \frac{2(1-\nu)}{1-2\nu}\frac{\mu_\infty}{E_f}\frac{1}{k^2 H h_f}\right]^{1/2} \quad (24)$$

which is valid only if the bilayer is unstable and there is a nonzero real-valued equilibrium amplitude of the corrugation. Moreover, minimizing the elastic stress energy in the bilayer with respect to the wavenumber leads to the next equilibrium corrugation wavelength:

$$L_{eq} = \pi h_f \left[\frac{2(1-2\nu)}{3(1-\nu)(1-\nu_f^2)}\frac{E_f}{\mu_\infty}\frac{H}{h_f}\right]^{1/4} \quad (25)$$

Comparing (25) with the fastest growing wavelength (21), it can be noted that they can be completely independent. The fastest growing wavelength, which dominates the initial growth, is determined by kinetics and depends on the compressive stress σ_0 in the elastic layer but does not depend on the viscoelastic layer. The equilibrium wavelength, on the contrary, is determined by energy and depends on the thickness and elastic modulus of the viscoelastic layer but does not depend on the stress in the elastic layer. This independence makes it possible to simultaneously determine the residual stress σ_0 and the modulus of elasticity μ_∞ from the initial and final corrugation wavelengths, respectively.

Indeed, from the kinetics of the process, we find by formula (23) the critical value $\sigma_0 = \sigma_0^c$, below which the bilayer is stable. Substituting $\sigma_0 = \sigma_0^c$ into (21) and equating the right-hand sides of expressions (21) and (25), we find

$$\mu_\infty = \frac{3(1-\nu_f^2)(1-2\nu)}{2(1-2\nu)}\frac{(\sigma_0^c)^2}{E_f}\frac{H}{h_f}. \quad (26)$$

In a state of equilibrium, the shear displacement on the surface is close to zero, and the lateral displacement is approximately described by the formula

$$u = \frac{1}{8}kA_{eq}^2 sin(2kx), \quad (27)$$

where $k = 2\pi/L_{eq}$. Thus, the in-plane displacement wavelength is equal to half the corrugation wavelength at equilibrium.

When the "film-substrate" system is cooled, the surface layer of the polymer coating is cured, which is accompanied by its

shrinkage information. In this case, tensile internal stresses develop in the cured layer, which generate deformations of the interface when the system is loaded. In this case, the distribution of stresses and strains at the interface "surface layer - substrate" appears in the form of modes of the "chess-board" or "herring bone" type [39].

These modes were considered in [39] based on the analysis of classical bends of a rigid substrate using a linearized analysis of stability.

Let E, ν, α and E_s, ν_s, α_s – Young's modulus, Poisson's ratio and thermal expansion coefficient of the film and substrate, respectively; t-film thickness. Let us assume that the substrate is much thicker than t and creates in-plane stresses in the film. Further, it is assumed that during the deposition of the film on the substrate, both of them have a temperature T_D and after deposition the temperature of the system will change by ΔT. In addition, the film is considered elastic and initially free of deformation. Then the compressive axially symmetric in two directions stress of the film will be

$$\sigma_{11} = \sigma_{22} = -\sigma_0 = -[E/(1-\nu)] \int_{T_D-\Delta T}^{T_D} \Delta\alpha dT, \quad (28)$$

where $\Delta\alpha = \alpha_s - \alpha$. Consider the case $\Delta\alpha > 0$ and $\sigma_0 > 0$.

According to the theory of Karman plates [44], the deflection of the film from the plane (deflection) w satisfies the equations:

$$D\nabla^4 w - (N_{11}w_{\cdot 11} + N_{22}w_{\cdot 22} + 2N_{12}w_{\cdot 12}) = -p \quad (29)$$

$$\frac{1}{Et}\nabla^4 F = w_{\cdot 12}^2 - w_{\cdot 11}w_{\cdot 22}. \quad (30)$$

Here, ∇^4 – a biharmonic operator; $\mathrm{D} = \mathrm{Et}^3/[12(1-\nu^2)]$ - bending stiffness of the plate; w-offset perpendicular to the plane (x_1, x_2); p – a component of stress, acting perpendicular to the plate under the influence of the substrate; $(w)_{\cdot\alpha} \equiv \partial(\sigma_\alpha)/\partial x_\alpha; N_{\alpha\beta} = \int \sigma_{\alpha\beta} dx_3$ – the resultant force acting in the plane of the plate; F – Airy stress, for which $N_{11} = F_{\cdot 22}, N_{22} = F_{\cdot 11}, N_{12} = -F_{\cdot 12}$. Equality (29) represents the equilibrium moment equation, and (30) the compatibility equation ensuring the existence of the gradient shift in the plane, $u_{\alpha\beta}$. We will neglect the tangent components of the traces that appear on the plate under the action of the substrate. This is a standard approximation for the analysis of corrugation of a thin film under the influence of a substrate [46], the accuracy of which can be verified by detailed analysis of one-dimensional modes. The average surface stress associated with plate displacements is represented as

$$E_{\alpha\beta} = \frac{1}{2}\left(u_{\alpha,\beta} + u_{\beta,\alpha}\right) + \frac{1}{2}w_{\cdot\alpha}w_{\cdot\beta};$$

$$N_{\alpha\beta} = [E/(1-\nu^2)]\ \mathrm{x}$$

$$\mathrm{x}\ \left((1\text{-}\nu)\mathrm{E}_{\alpha\beta} + \nu\mathrm{E}_{\gamma\gamma}\delta_{\alpha\beta}\right);$$

$$\mathrm{M}_{\alpha\beta} = \mathrm{D}\left((1\text{-}\nu)\mathrm{w}_{\cdot\alpha\beta} + \nu\cdot\mathrm{w}_{\cdot\gamma\gamma}\delta_{\alpha\beta}\right) -$$

non-adjustable ratios representing the moment of the bend tensor.

In the absence of bends, the film has a state of uniform stress, determined by the equalities $N_{11} = N_{22} = -\sigma_0 t$, $N_{12} = 0$. The classical bend analysis based on linearization of equations (29) and (30) leads to the equations

$$D\nabla^4 w + \sigma_0 t\nabla^2 w = -p \quad (31)$$

$$\nabla^4 \Delta F = 0, \quad (32)$$

$F = -\frac{1}{2}(x_1^2 + x_1^2)\sigma_0 t + \Delta F$. The system of equations (31) - (32) has periodic solutions

$$w = \hat{w}cos(k_1 x_1)cos(k_2 x_2),$$

$$p = \hat{p}cos(k_1 x_1)cos(k_2 x_2), \qquad (33)$$

at which equation (31) takes the form

$$(D \cdot k^4 - \sigma_0 t k^2)\hat{w} = -\hat{p}, \qquad (34)$$

where $k = \sqrt{k_1^2 + k_2^2}$.

For an infinitely deep substrate under normal load p in (29), provided that there are no tangent traces on the surface, the exact solution for the normal deviation, δ, has the form

$$\delta = \hat{\delta}\cos(k_1 x_1)cos(k_2 x_2), \qquad (35)$$

where $\hat{\delta} = 2\hat{p}/(\bar{E}_s k)$ c $\bar{E}_s = E_s/(1 - \nu_s^2)$.

The effect of the boundary conditions on the displacements along the tangential directions to the substrate surface is insignificant and therefore neglected. Under the condition $\hat{w} = \hat{\delta}$ from equation (34) and $\hat{\delta} = 2\hat{p}/(\bar{E}_s k)$ we obtain the equation for the eigenvalues k:

$$\sigma_0 t = Dk^2 + \bar{E}_s/2k \qquad (36)$$

The critical value of the bending stress, σ_0^c, which is the minimum over k of equation (36), attained at

$$k^c \cdot t = (3\bar{E}_s/\bar{E})^{\frac{1}{3}}, \qquad (37)$$

defined by the expression

$$\sigma_0^c = \frac{1}{4}\bar{E}(3\bar{E}_s/\bar{E})^{2/3}, \qquad (38)$$

where $\bar{E} = E/(1 - \nu^2)$.

The right-hand sides of formulas (3) and (38) coincide. However, formula (38) was obtained for the residual stress σ_0 in the initial state of the film and, moreover, σ_0 can be much larger than the critical value σ_0^c (see Fig. 2).

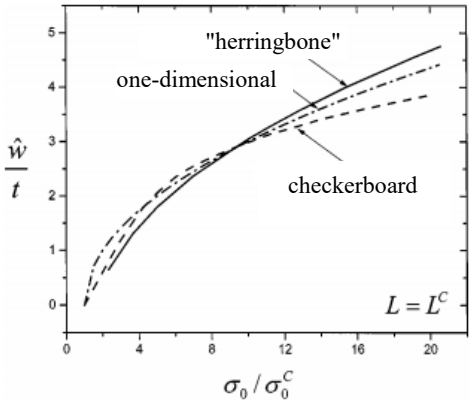

Figure 2 – The dependence of the bending amplitude of a thin layer, $\hat{w}_1/t$, is considered as a function of σ_0/σ_0^c for three modes. The wavelength (and slope in the case of the herringbone pattern) corresponds to its critical value at the onset of bending deformation.

Equality (38) is valid for a one-dimensional stress that causes corrugation with plane tension. This fact is well known [46]. In the case of a biaxially symmetric stress, the critical stress is applicable only for a one-dimensional mode with $k_1 = k^2$ and $k_2 = 0$, but for any mode the wavenumbers must satisfy the equality

$$\sqrt{k_1^2 + k_2^2} \cdot t = k^c \cdot t = (3\bar{E}_s/\bar{E})^{\frac{1}{3}}. \qquad (39)$$

As shown in [39], nonlinear tensile displacements of the substrate essentially do not affect the behavior of the film. It is believed that the substrate has a very large thickness d, comparable to the wavelength of the mode, and on its lower surface the normal and tangential displacements are zero. It is assumed that the difference between the thermal expansion coefficients of the film and the substrate is $\Delta\alpha$,

and the difference between their temperatures in the initial unloaded state is ΔT.

The biaxial compressive stress in an unbent film will therefore be equal to $\sigma_0 = E\Delta\alpha\,\Delta T/(1-\nu)$ if the substrate is very thick.

Let us consider square modes of the "checkerboard" type ("check board mode" in the terminology of [39]) with a wavelength L in the x_1 and x_2 directions, determined by the critical condition (37);

$2\pi/k_1 = 2\pi/k_2 = L = \sqrt{2}\cdot L^C$, $L^C = 2\pi/k^C$C. The "checkerboard" cell in this case is a rectangular parallelepiped of dimension $L \times L \times d$.

A very small initial deformation, predetermined by the fact that the uncompressed system at $\Delta T = 0$ has a weak average surface deviation, is written in the form

$$w = \widehat{w}_l \cos(k_1 x_1) cos(k_2 x_2), \qquad (40)$$

where $\widehat{w}_l/t = 0{,}02$.

The periodicity conditions applied to a cell as a result of all five nodal degrees of freedom are the same on both sides of the cell parallel to the x_1 axis and similarly for the x_2 axis. In addition, at each corner of the cell, the conditions $\partial w/\partial x_1 = 0$ and $\partial w/\partial x_2 = 0$ lead to the fact that the rises alternate with dips on the sides of the cell.

Modes of the "checkerboard" type are indeed determined by deviations along the normal, approximately described by the equations

$$w = \widehat{w}\cos(k_1 x_1) cos(k_2 x_2) \qquad (41)$$

The numerical relationship between the amplitude of the mode, $\widehat{w}/t$, defined as the half-difference between the maximum and minimum deviations, and the ratio σ_0/σ_0^c is illustrated in Fig. 2 [39].

Fig. 2 shows that the deviations of the one-dimensional mode lie between the deviations of the "checkerboard" and "herringbone" modes.

As shown in [39], the minimum of the configuration energy is attained at $L/L^C \cong 1$, and under this condition, the deflection along the normal has a herringbone mode.

A typical image of such a mode is shown in Fig. 3 [39].

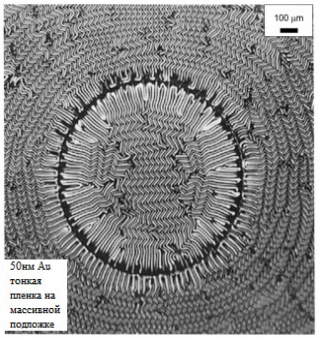

Figure 3 – A gold thin film on a substrate having a pattern with a circular flat depression a few millimeters in diameter. A herringbone pattern appears in the center of the cell outside the edge of the spot.

Nonlinear waves of localized plastic flow

The clearest physical meaning of the "checkerboard" distribution of stresses and strains in a thin film was obtained in [47], where the theoretical substantiation of the mechanism of the interface between the film and the substrate was given for the first time.

According to the authors, the curing of the paint and varnish coating (PVC) leads to the formation of a kind of surface layer of the substrate in the form of a thin film lying on the substrate. This surface layer, according to the concept of physical mesomechanics, is an independent subsystem in a deformable (under the influence of external load) solid. The interface in the thin film-substrate system is of particular interest.

First, when a thin film is coupled to a substrate, a pronounced interface is formed, on which a geometrically correct “checkerboard” distribution of stresses and strains is realized, and the thickness of the film can be taken as the interface thickness in theoretical analysis.

Second, a thin film is a highly nonequilibrium system. This is due both to its highly developed surface at a small volume and to a mismatch at the interface of the mating media (with different elastic moduli and thermal expansion). As a consequence, a nonequilibrium thin film in the initial state should have a cluster structure that will use structural-phase transitions in the fields of external influences of any nature [2]. A wide range of atomic configurations in the resulting surface layer causes the development of more intense plastic deformation in it than in the bulk of the crystal. The necessity of compatibility of the processes of plastic flow of the surface layer and the crystalline substrate causes the appearance of a quasiperiodic distribution of stresses and strains at the interface (their interface).

The analysis of theoretical and experimental studies carried out in [47] on the development of a localized plastic flow in the form of double spirals in nanostructured layers of a deformable solid led to the conclusion that the interface of dissimilar media in a two-dimensional dimension should have the form of a "checkerboard". Modeling the interface "surface layer-substrate" in a loaded solid, carried out in [48, 49, 29] on the basis of a stochastic approach in the framework of a three-dimensional model, confirmed the conclusion [47] about the "checkerboard" distribution of local stresses and strains when two dissimilar media are coupled.

Received theoretical confirmation and explanation of the channeling effect of local plastic flow in nanostructured surface layers along the cells of the "checkerboard" interface structure with tensile normal stresses.

Direct experimental confirmation of the "checkerboard" character of the distribution of stresses and strains at the interface "surface layer-base crystal" was obtained in [50] on the example of an experimental study of alternating bending of flat samples of polycrystalline VT1-0 titanium with a hydrogenated surface layer. The "checkerboard" character of stress distribution at the interface "nanostructured surface layer - the main volume of material" provides the effect of plastic flow channeling and extrusion of the surface material in the form of double spirals of intertwining mesobands of localized deformation (Fig. 4 [51]). As a result, deformation defects reach the surface, rather than being pumped into the depth of the loaded sample. The latter retards the development of deformation macro-localization in the sample, causing a simultaneous increase in both the strength and plasticity of the material.

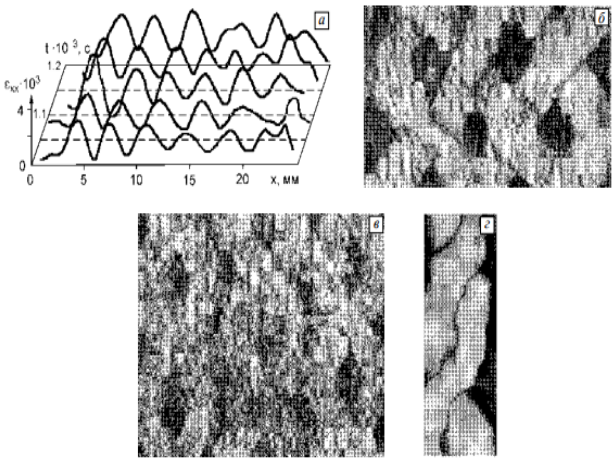

Figure 4 – The experimental pictures of stationary corrugation of the surface layer in a deformable solid; tension at 293 K: a – a polycrystalline alloy Zr – 2.5% Nb; b, c, d – low-carbon St3; stretching at T=293K after ultrasonic treatment and subsequent annealing at T=1103K; ε=13 (b), 28 (c), 32% (d); scanning electron microscopy, x250.

The cells of the "checkerboard" distribution of tensile and compressive normal stresses determine the corresponding cellular structure of the distribution of material in a thin film: the material from the cells of compressive normal stresses is displaced into the cells of tensile normal stresses.

Mass transfer occurs in the field of shear stresses, which also have a "checkerboard" distribution at the interface but are phase-shifted by $\pi/2$ in space.

Stochastic approach to calculating internal stresses and strains. Since the film is rigidly bound to the substrate, then under loading up to the beginning of fracture, both the film and the substrate should experience the same degree of deformation. Hence it follows that elastic stresses in the film σ_f are related to stresses in the substrate σ_s as follows

$$\sigma_f = \frac{1-\nu_s^2}{1-\nu_f^2}\frac{E_f}{E_s}\sigma_s, \qquad (42)$$

where E_f, E_s, , ν_f and ν_s – Young's moduli and Poisson's ratios of the film and substrate material, respectively.

Due to the small grain size and high density of grain boundaries, dislocation plasticity in nanostructured films is limited. As a result, deformation develops at the mesoscale level under the conditions of a "checkerboard" stress distribution at the "film-substrate" interface, while the role of the maximum shear stresses, which determine the directions of shears in the deformed film, significantly increases.

Since plastic deformation can occur only in the region of tensile normal stresses [47, 51], when thin films are stretched, meso-bands of localized deformation develop, decorating the “checkerboard” structure of the interface.

The conjugation of the modified surface layer and the substrate in a loaded solid causes two types of perturbations: nanoconfigurational perturbations of the atomic structure at the interface between two dissimilar media, such as atomic clusters of different configurations, and a sinusoidal field of tensile and compressive elastic stresses in the surface layer due to the inequality of the elastic moduli of the surface layer and the substrate.

Self-organization of nanoconfigurational perturbations at the interface "modified surface layer - substrate" in a sinusoidal elastic field of change in tensile and compressive normal stresses in the surface layer causes a "checkerboard" distribution of stresses and inelastic deformations in the surface layer.

Figure 5 [52] shows the evolution of the "checkerboard" organization of atomic configurational perturbations at the interface "modified surface layer - substrate" in a three-dimensional elastic field of the surface layer with a sequential increase in the degree of deformation of the sample in the range 0.01...0.5%.

The dark areas in Fig.5 correspond to the zones of compressive normal stresses, and the light ones correspond to the zones of tensile stresses.

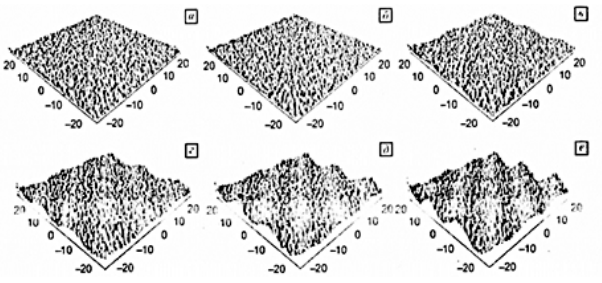

Figure 5 – Pattern of inelastic deformation of the surface layer at different degrees of uniaxial tension of the

sample: ε=0.01 (a); 0.05 (b); 0.1 (c); 0.2 (g); 0.3 (d); 0.5% (e)

The need to interface the surface layer with a substrate that exhibits higher shear stability leads to corrugation of the surface layer. The character of this corrugation changes in stages as the degree of deformation increases. Figure 6 [29] shows a pattern of corrugation of the surface layer of various thicknesses depending on the length l_x of the film section under consideration.

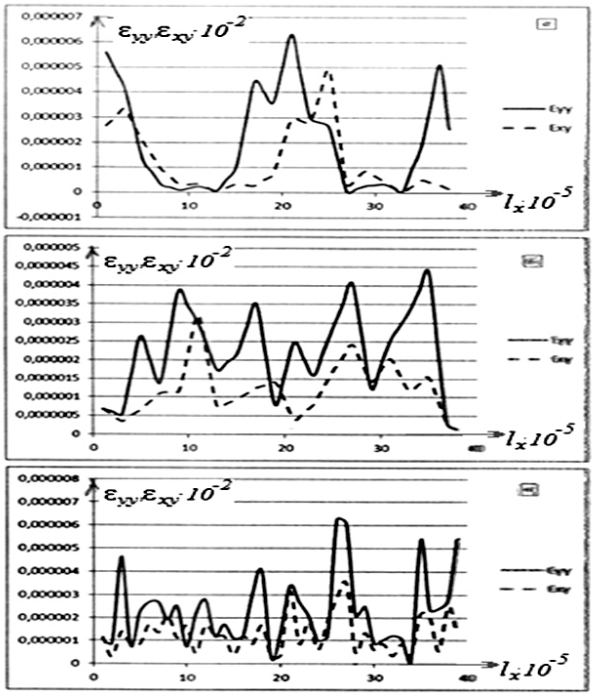

Figure 6 – Profiles of normal ε_{yy} and tangential ε_{xy} deformation components depending on the length l_x at the interface thickness of 10^{-6} (a), 10^{-7} (b), and 10^{-8} (c) m.

The normal $\sigma(x_i)$ and tangential $\tau(x_i)$ stress components at the point x_i of the simulated section of the film/substrate interface are represented by the following expressions:

$$\sigma(x_i) = (E_z(x_i) - \alpha T)E, \quad (43)$$

$$\tau(x_i) = \big(E_y(x_i) - \alpha T\big)G, \quad (44)$$

where $x_i = i \cdot l_x/n$, $i = 0,1,\dots,n$ – the set of dividing points of the considered section $[0, l_x]$ of the film; E and G – moduli of elasticity and shear of the substrate; T – temperature of the simulated section of the interface; α is the coefficient of linear thermal expansion of the substrate material; $E_z(x_i)$ and $E_y(x_i)$ values at $s = x_i$ of deformation diagrams $E_z(s)$ and $E_y(s)$, which under symmetry conditions imposed on deformations at the boundaries of the deformable region

$$E_u(L) = E_u(-L), \quad u = x, y, z, \quad (45)$$

have the form:

$$E_x(s) = 0;\ E_y(s) = L\left(sech\frac{2s}{L} - 1\right);$$
$$E_z(s) = s - L \cdot tgh\frac{2s}{L} \quad (46)$$

and do not depend on time; thz and $sechz$ – the hyperbolic tangent and secant functions:

$$thz = (e^z - e^{-z})/(e^z + e^{-z}),$$

$$sechz = 2/(e^z + e^{-z}).$$

Normal $\varepsilon_{yy}(x_i)$ and tangential $\varepsilon_{xy}(x_i)$ deformation profiles are determined by the formulas

$$\varepsilon_{yy}(x_i) = E_z(s)|_{s=x_i},$$

$$\varepsilon_{xy}(x_i) = E_y(s)\big|_{s=x_i}. \quad (47)$$

Based on the measured parameters, the level of internal stresses was calculated using formula (43).

Results and its discussion

The deflection of the steel console with PES coating was $d = 285.47\mu m$. The results of measuring the film thickness before and after curing showed that the initial average

thickness of the "wet" film was $h_0 = 51.21\mu m$, and after curing $h_1 = 47.06\mu m$.

The results of AFM studies of the microrelief (profilograms) and volumetric topography of the surface of the PES film showed that the mean wavelength of the corrugation is $\lambda = 1.25\mu m$ with an amplitude of $A = 96nm$

Since the total thickness of the coating ($H = h1 = 47.06\mu m$) is more than 35 times the length of the RMR wavelength ($\lambda = 1.25\mu m$), it can be assumed that the thickness is much greater than the lengt h (Figure 7).

Considering the roughness profile in the framework of multifractal analysis, it can be noted that it has the property of invariance, when the same elementary geometric object (in our case, a straight cone) is continuously repeated over the entire area of the investigated area [35].

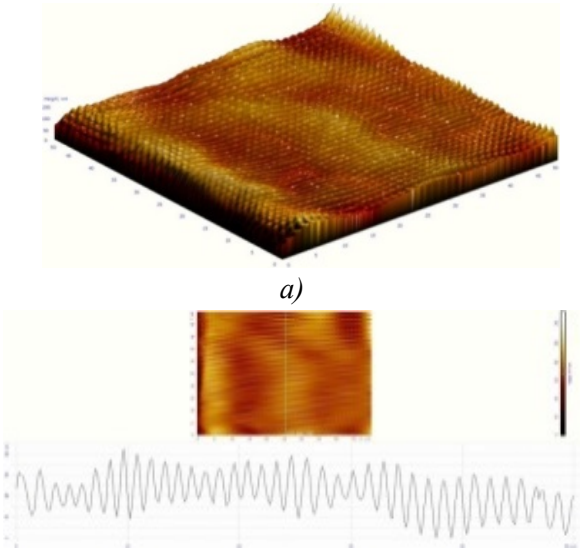

a)

b)

Figure 7 – The volumetric topography (a) and average micro-profile (b) of the sample (50 × 50μm) of polyester urethane varnish.

After measuring all the parameters using formulas (1), (2), and (43), the internal normal stresses in the PEUL film were calculated (Table).

Table. The values of the internal stresses of the PES film, determined by different methods

Method	Internal stress, MPa
Cantilevered [12]	2.921
Thickness difference [13]	2.431
RMR parameters measu-ring	2.626

As follows from the table, the internal stresses measured by all three methods are relatively the same and amount to about $\sim 0.1E$, the difference between the obtained values does not exceed $\sim 20\%$.

However, despite the fact that measurements of internal stresses by three methods give close values, the proposed method is much simpler than the other two in terms of convenience.

The advantage of this method is the ability to evaluate internal stresses in a polymer film solely by the geometric characteristics of the cured profile irregularities (wavelength, amplitude, thickness), without the need to measure the "wet" coating thickness and regardless of the mechanical properties and dimensions of the substrate.

After curing the polymer film at low temperatures, the calculations assumed that the thickness h of the elastic film and the thickness H of the underlying viscoelastic layer are small values of the same order, forming a kind of surface layer of the bulk of the substrate, which we conditionally called a "thin film". The film thickness is taken as the thickness of the surface layer / substrate interface, which makes it possible to compare the results of experimental studies with models of physical mesomechanics of heterogeneous media.

Measurements of the parameters of the regular microrelief (RMR) of the film surface make it possible to describe the kinetics of film formation and growth and to estimate the total

energy level of the film/substrate system with the calculation of the critical values of the amplitude and wavelength of nonlinear film vibrations at which their stability appears, providing certain steady-state, independent from time to time, the values of the amplitude and wavelength of oscillations with the corresponding formed profile of deformations on the surface of the film.

The real conditions for curing the paintwork (PVC) are a random process. In this regard, the distribution of stresses and strains at the film / substrate interface is naturally modeled on the basis of a stochastic approach [49, 50]. The introduction of stochastics is due to the fact that, within the framework of this approach, the elements of the medium of the mesoscale level are considered, the physical parameters of which (such as temperature, pressure, elastic moduli) cannot be measured "absolutely accurately", as for objects of the macrocosm. At the micro level, their own laws operate, there it is impossible to unambiguously determine the parameters of physical objects, they can only be spoken of as interconnected random variables. It should be noted that the mesoscale level is a connecting and directly determining link in the system of factors that affect the behavior of surfaces and interfaces of a deformable solid.

Conclusion

It is shown that the contact of the cured coating with the elastic base can be considered as the interface of the surface layer in the form of a thin film of paintwork varnish with the bulk of the substrate material.

The loading of the substrate solid causes the distribution of stresses and strains on the outer surface of the film in the form of a "checkerboard" effect. As a result, deformation defects emerge on the surface and are not pumped into the depth of the loaded specimen, thereby retarding the development of deformation macro-location in the specimen, causing a simultaneous increase in the strength and plasticity of the specimen material.

The proposed method for assessing internal stresses based on measuring the parameters of the regular microrelief (RMR) of the film surface makes it possible to describe the kinetics of film formation and determine the critical values of the main characteristics of vibrations, which can be used to reveal stability.

To calculate internal stresses and strains, a stochastic approach was used, which takes into account the peculiarities of the flow of the film / substrate interface at the meso- and microscale levels, caused by the uncontrollability of external conditions affecting the properties of the sample. The values of the shrinkage stresses of the polyester urethane coating, calculated by the proposed and cantilever methods, by the method of thickness difference, are relatively the same (the difference does not exceed $\sim 20\%$) and are of the order of $\sim 0.1E$.

REFERENCES

1. **Uglov A.A. i dr.** Adgezionnaya sposobnost plyonok. - M.: *Radio i svyaz*, 1987. S. 28-32 (in Russia).
2. **Panin V.E., Panin A.V., Sergeev V.P., Shugurov A.R.** Effekty skejlinga v strukturno-fazovoj samoorganizacii na interfejse «tonkaya plyonka – podlozhka» // *Fizicheskaya mezomekhanika*, 2007, t. 10. №3. S. 9-21(in Russia).

3. **Lihua Jin, Atsushi Takei, John W.** Hutchinson. Mechanics of wrinkle/ridge transitions in thin film/substrate systems // *Journal of the Mechanics and Physics of Solids*. Vol. 81, August 2015, Pp. 22-40.
4. **Sanzharovskij A.T.** Metody opredeleniya mekhanicheskih i adgezionnyh svojstv polimernyh pokrytij. M.: *Nauka,* 1974, s. 6 (in Russia).
5. **Suhareva L.A.** Dolgovechnost polimernyh pokrytij. – M.: *Himiya,* 1984. – 240 s. (in Russia).
6. **Epifanov G.I., Moma Y.A.** Fizicheskie osnovy konstruirovaniya i tekhnologii REA i EVA. Uchebnoe posobie dlya vuzov. M.: *Sovetskoe radio*, 1979, s. 85 (in Russia).
7. **Petrova A.P.** Termostojkie klei. M.: *Himiya*, 1977, s. 9 (in Russia).
8. **Tadmor Z., Gogos K.** Teoreticheskie osnovy pererabotki polimerov, M.: *Himiya,* 1984, 632 s. (in Russia).
9. **Sanzharovskij A.T.** Vnutrennie napryazheniya v pokrytiyah. Vysokomolekulyarnye soedineniya, t. 2, №11, 1960, s. 1698-1702. (in Russia).
10. Fizika tonkih plyonok. Pod red. G. Hassa. T. 1, per. s angl., M.: *Mir,* 1967, s. 245 (in Russia).
11. **Corcoran E.M.** Determining Stresses in Organic Coatings using Plate Beam Deflection // *Journal of Paint Technology.* Vol. 41, No. 538. November 1969.
12. GOST 13036-67 Laki i kraski. Metod opredeleniya vnutrennih napryazhenij v lakokrasochnyh pokrytiyah. (in Russia).
13. ASTM D6991-05: Standard Test Method for Measurements of Internal Stresses in Organic Coatings by Cantilever (Beam) Method. ASTM International, 100 Barr Harbor Drive, PO Box C700, West Conshohocken, Pennsylvania, USA 19428-2959.
14. **Zinovjev V.E., Harlamov P.V.** Vliyanie mikrotreshchin, skrytyh defektov i ostatochnyh napryazhenij polimernogo kleevogo sloya na ego razrushenie // *Fundamental'nye issledovaniya*, 2015, № 12-1, s. 37-42 (in Russia).
15. **Pashaev A.M., Mekhtiev A.Sh., Nizamov T.I. i dr.** Uplotnitel'nyj kompaund. Patent AR I 20060022. (in Russia).
16. **Dragunov Yu.G., Zubchenko A.S., Kashirskij Yu.V. i dr.** Marochnik stalej i splavov. 4-e izd., pererabot. i dop. – M.: 2014. 1216 s.: ill. (in Russia).
17. GOST 31993-2013 (ISO 2808:2007) Materialy lakokrasochnye. Opredelenie tolshchiny pokrytiya. (in Russia).
18. ASTM D4114-95. Standard Practice for Measurements of Wet-Film Thickness by Notch Gauges.
19. ASTM D1212-91 (2013). Standard Test Methods for Measurement of Wet Film Thickness of Organic Coatings
20. OST 1 02507-92 Samolety dozvukovye. Obshchie trebovaniya k kachestvu vneshnej poverhnosti (in Russia).
21. **Yakovlev A.D.** Himiya i tekhnologiya lakokrasochnyh pokrytij. S-Pb.: *Himizdat,* 2008. – 448 s., il. (in Russia).
22. **Rozenfeld I.L., Rubinshtejn F.I., Zhigalova K.A.** Zashchita metallov ot korrozii lakokrasochnymi pokrytiyami. M., *Himiya*, 1987 g., 224 s. (in Russia).
23. **Jan Genzer, Jan Groenewold.** Soft matter with hard skin: From skin wrinkles to templating and material characterization // Soft Matter, 2, 310–323 (2006)
24. **E. Cerda1, L. Mahadevan.** Geometry and Physics of Wrinkling // Physical Review Letters 90 (7), pp. 074302/1-074302/4 (2003)
25. **Richard Vendamme, Takuya Ohzono, Aiko Nakao, Masatsugu Shimomura, Toyoki Kunitake.** Synthesis and Micromechanical Properties of Flexible, Self-Supporting Polymer-SiO2 Nanofilms // *Langmuir*, 23, 2792-2799 (2007)
26. **Volynskij A.L., Bakeev N.F.** Strukturnaya samoorganizaciya amorfnyh polimerov – M.: Fizmatlit, 2005, 230 s. (in Russia).
27. **Takashi Nishino, Akiko Nozawa, Masaru Kotera, and Katsuhiko Nakamae.** In situ observation of surface deformation of polyimide film // Journal of the Society of Rheology, Japan, 32, 4, 211-214 (2004)
28. Fizicheskaya mezomekhanika i komp'yuternoe konstruirovanie materialov. Pod red. Panina V.E. T. 1, Novosibirsk: Nauka, 1995, 298 s. (in Russia).
29. **Pashaev A.M., Janahmadov A.Kh., Dyshin O.A.** Stohasticheskij podhod k resheniyu zadachi o deformacii granicy razdela v nagruzhennom tverdom tele // Vestnik Azerbajdzhanskoj inzhenernoj akademii, t. 9, №2, 2017, s. 34-47(in Russia).
30. **Xiaodong Li, Weijie Xu, Michael A. Sutton, and Michael Mello**. In Situ Nanoscale In-Plane Deformation Studies of Ultrathin Polymeric Films During Tensile Deformation Using Atomic Force Microscopy and Digital Image Correlation Techniques // *IEEE Transactions on Nanotechnology*, 6, 1, 4-12 (2007)

31. Mashinostroenie. Enciklopedicheskij spravochnik pod red. Chudakova E.A. Razdel 1. Inzhenernye raschety v mashinostroenii. V 15-ti tt. T.1. Glavnoe nauchno-tekhnicheskoe izd-vo mashinostroitel'noj lit-ry. M. 1947, s. 428 (in Russia).
32. **Leocmach M., Nespoulous M., Manneville S., Gibaud T.** Hierarchical wrinkling in a confined permeable biogel. Science Advances, v.1(9), 2015.
33. **Shugurov A.R., Panin A.V.** Mekhanizmy periodicheskoj deformacii sistemy «plyonka-podlozhka» pod dejstviem szhimayushchih napryazhenij// *Fizicheskaya mezomekhanika*, №12 (3), 2009 g., s. 23-32 (in Russia).
34. **Krauford F.** Berkleevskij kurs fiziki. Tom 3. Volny. M.: *Nauka*, 1974, s. 315 (in Russia).
35. **Pashaev A.M., Janahmadov A.Kh.** Fraktal'nye podhody v mekhanike razrusheniya. – Baku: *Apostroff*, 2015, 440 s. (in Russia).
36. **S.H. Im., R. Huang,** Evolution of wrinkles in elastic-viscoelastic bilayer thin films //J. *Appl. Mech*., v.72, pp. 955-962 (2005).
37. **R. Huang.** Kinetic wrinkling of an elastic film on a viscoelastic substrate // J. *Mech. Phys. Solid*, v.53, pp.63-89 (2005).
38. **J. Groenewold,** Wrinkling of Plate s Coupled With Soft Elastic Media // *Physica A.,* 298, pp.32-45 (2001).
39. **X. Chen and J.W.** Hutchinson, Herringbone Buckling Patterns of Compressed Thin Films on Compliant Substrates // J.*Appl. Mech*., 71, pp. 597-603 (2004).
40. **Z.Y. Huang, W.Hong and Z. Suo,** Nonlinear Analysis of Wrinkles in Films on Soft Elastic Substrates // J.Mech. Phys. Solids, 53, pp.2101-2118 (2005).
41. **N. Shridhar, D.J. Srolovitz, and Z. Suo,** Kinetics of Buckling of a Compressed Film on a Viscous Substrate // *Appl. Phys. Lett.,* 78, pp.2482-2484 (2001).
42. **R. Huang and Z. Suo,** Wrinkling of an Elastic Film on a Viscous Layer // J. Appl. Phys. 91, pp.1135-1142 (2002).
43. **P.J. Yoo, and H.H. Lee,** Evolution of a Stress – Driven Pattern in Thin Bilayer Films: Spinodal Wrinkling // *Phys. Rev. Lett*. 91, 154502 (2003).
44. **S.P.Timoshenko, J.M.Gere,** Theory of Elastic Stability, Mc Graw – *Hill*, New York, 1961.
45. **R.M. Christinesen**. Theory of Viscoelasticity: An Introduction. Academic Press, New-York, 1982.
46. **H.G. Allen.** Analysis and Design of Structural Sandwich Panels, Pergamon, New-York, 1969.
47. **Panin A.V.** Nelinejnye volny lokalizovannogo plasticheskogo techeniya v nanostrukturirovannyh poverhnostnyh sloyah tverdyh tel i tonkih plenkah. //*Fiz. mezomekh*. 2005. T.8. №3. S.5-17 (in Russia).
48. **Moiseenko D.D., Maksimov P.V., Solovyev I.A.** Stohasticheskij podhod k mnogourovnevomu modelirovaniyu vozmushchenij na granicah razdela v nagruzhennom tverdom tele //*Fiz. mezomekh*. 2004. T.7. №2. S.19-24 (in Russia).
49. **Moiseenko D.D., Maksimov P.V**. Raspredelenie napryazhenij i deformacij na interfejse «poverhnostnyj sloj – podlozhka»: modelirovanie na osnove stohasticheskogo podhoda //*Fiz. mezomekh*. 2005. T.8. №6. s.89-96 (in Russia).
50. **Panin V.E., Panin A.V., Elsukova T.F., Kuzina O.Y.** Effekt «shahmatnoj doski» v raspredelenii napryazhenij i deformacij na interfejsah v nagruzhennom tverdom tele: Eksperimental'naya verifikaciya i mekhanizmy mezoskopicheskogo kanalirovaniya //*Fiz. Mezomekh*. 2005. T. 8. №6. S. 97-105 (in Russia).
51. **Panin V.E., Panin A.V.** Effekt poverhnostnogo sloya v deformiruemom tverdom tele // *Fiz. mezomekh*. 2005. T.8. №5. S.7-15 (in Russia).
52. **Panin V.E., Panin L.E.** Masshtabnye urovni gomeostaza v deformiruemom tverdom tele // *Fiz. mezomekh*. – 2004. –T.7 - №4. - S.5-24 (in Russia).

Received: *20.11.2020*
Revised: *12.06.2021*
Accepted: *20.06.2021*